Proceedings of the ASME 2013 Summer Bioengineering Conference
SBC2013
June 26-29, 2013, Sunriver, Oregon, USA

SBC2013-14405

EFFECT OF THE ANASTOMOTIC ANGLE ON THE WALL SHEAR STRESS PROFILES IN THE ARTERIOVENOUS FISTULAE

Briana M. Conners[1], Ehsan Rajabi-Jaghargh[2], Rupak K. Banerjee[2]

[1]Chemical Engineering Program, School of Energy, Environmental, Biological and Medical Engineering, University of Cincinnati, Cincinnati, OH

[2]Mechanical Engineering Program, School of Dynamic Systems, University of Cincinnati, Cincinnati, OH

ABSTRACT

A significant number of arteriovenous fistulae (AVFs) fail to mature to support hemodialysis. Hemodynamic parameters, mainly wall shear stress (WSS), are believed to play a crucial role in the maturation or failure of AVFs. Our *goal* is to study the effects of the AVF configuration on the WSS profile. Idealized AVFs with 90°, 60°, and 30° anastomotic angles were created based on our previous experimental data from an *in-vivo* swine model [1]. The hemodynamic parameters were then obtained using numerical techniques under steady state condition. The average WSS values for our models were within range of the swine model average WSS (=174.9±64.6 dyne/cm^2). For all AVFs, WSS was higher along the bend. The highest WSS occurred on the outer wall (OW) of the 30° AVF (=613 dyne/cm^2) compared to the 60° (=407 dyne/cm^2) and 90° AVFs (=329 dyne/cm^2). WSS on the inner wall (IW) of the bend was negative with the smallest magnitude in the 90° AVF (=-91 dyne/cm^2) compared to the 60° (=-172 dyne/cm^2) and 30° AVFs (=-169 dyne/cm^2). In addition, the maximum difference in WSS (ΔWSS: measure of axial WSS gradient) was less for the 90° AVF (=158 dyne/cm^2) than the 60° (=170 dyne/cm^2) and 30° AVFs (=414 dyne/cm^2). A similar trend was found on the OW with ΔWSS of 161, 405, and 870 dyne/cm^2 for the 90°, 60°, 30° AVF, respectively. Moreover, AVFs with different angles can be categorized based on Dean number (*De*) which showed an inverse correlation to WSS range. Thus, creating an AVF with a surgical configuration that results in a low *De*, representing a sharp bend with large radius of curvature, could result in a hemodynamic condition (high WSS and ΔWSS) that could have adverse effects on the fistula maturation.

INTRODUCTION

Immediately after AVF creation, there is a multifold increase in the flow rate which causes a steep rise in WSS. In attempt to maintain pre-surgery conditions, the vessels respond to these hemodynamic changes by dilating [1]. However, the dilation and flow accommodation can be hindered by aggressive neointimal hyperplasia (NH) [2]. WSS, particularity extremely high or low values, has been shown to play an important role in the formation of NH. While hemodynamic changes after surgery are inevitable, the severity of the adverse effects from the changes can be affected by the AVF configuration.

The effects of surgical configuration on the corresponding hemodynamics within the access have mainly been studied on idealized

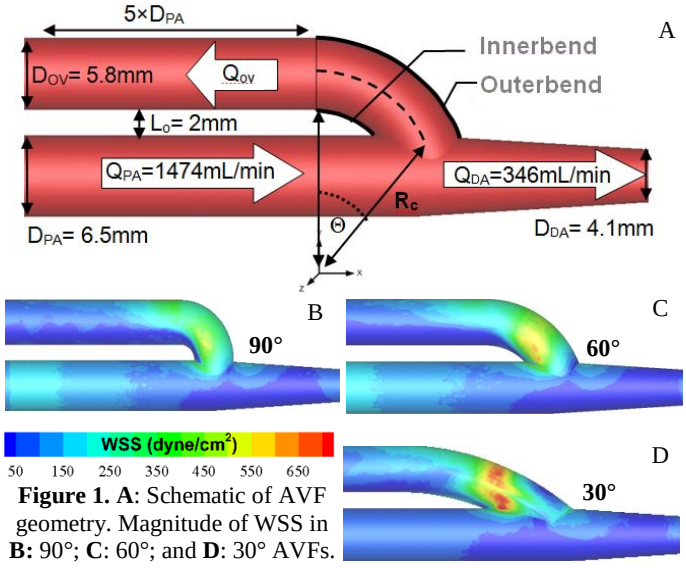

Figure 1. A: Schematic of AVF geometry. Magnitude of WSS in **B:** 90°; **C**: 60°; and **D**: 30° AVFs.

geometries [3]. These configurations were constructed based on simplified assumptions in which the outflow vein, proximal artery, and distal artery had identical diameters [3]. Therefore, in this study we tried to employ a more realistic AVF geometry based on the average dimensions of our *in-vivo* swine AVFs [2]. Our goal is to validate this idealized model with our data from the swine experiment and then categorize the geometrical effects on the WSS profiles within the AVFs using the Dean number.

METHODS

Three AVFs with 30°, 60°, and 90° angles were considered in our analysis. The schematic of the AVF geometry including the dimensions of the proximal (PA) and distal (DA) arteries, the outflow vein (OV), and the distance between the two vessels (L_o) are shown in Figure 1A. The flow rates at the PA (= 1474 ml/min) and DA (= 346 ml/min) had corresponding Reynolds numbers of 1464 and 508, respectively. These dimensions and flow rates were all chosen based on our *in-vivo* swine AVFs at 2 days post-surgery [1]. Radii of curvature for different cases varied based on the anastomotic angle and were 4.9, 9.8, and 36.6 mm for 90°, 60°, and 30° AVFs, respectively. To evaluate the flow field in the AVFs, an unstructured grid was generated, and the numerical domain was solved using control volume techniques under steady state condition. Velocity boundary conditions with parabolic profiles were applied at the PA and DA, and an outflow condition was specified at the OV. Also, in order to minimize the effects of boundary conditions on the AVF hemodynamics, all boundaries were extended using straight pipes with a length of 20D, where D was the diameter of the corresponding boundary.

RESULTS

Effects of Configuration on WSS Profiles. WSS contours are shown in Figures 1B-D. High WSS levels were noted along the outer wall (OW) of the bend, particularly in the 30° AVF which had the highest WSS levels among all the three cases. However, WSS was lower on the inner wall (IW) of the curve. Table 1 presents the average WSS across the entire AVF segment depicted in Figure 1 and the corresponding average WSS obtained from our swine model. For the models studied here, WSS values were within the 174.9 ± 64.6 dyne/cm^2 range obtained for the swine model in which no simplifications were made.

Table 1. Average WSS values across the entire AVF segment.

	Θ = 30°	Θ = 60°	Θ = 90°	Swine Model [1]
WSS (dyne/cm^2)	110.92	117.83	112.56	174.9 ± 64.6

Local Variation of WSS in the Bend Segment. The local variation of axial WSS along the inner wall (IW) and the outer wall (OW) of the three AVFs are shown in Figures 2A and 2B, respectively. Axial WSS at each boundary node was calculated through the dot product of WSS components and the corresponding unit vector in the axial direction. Here, axial WSS were of more interest than the overall WSS magnitude (Figure 1), as the axial WSS help align the endothelial cells in the direction of the flow. As shown in Figure 2A, for the 90° and 60° AVFs, WSS were negative along the majority of the IW indicating backward flow due to the formation of a recirculation zone. This characteristic was present only at the beginning of the curve in the 30° AVF. The average WSS on the IW of the 30° AVF was 144 dyne/cm^2, whereas it was -51 dyne/cm^2 and -53 dyne/cm^2, respectively, for the 90° and 60° AVFs. On the OW, negative WSS was only seen at the beginning of the 30° AVF. The average WSS on the OW was 216 dyne/cm^2 for the 30° AVF, which was lower than the average 256 dyne/cm^2 and 280 dyne/cm^2 for the 90° and the 60° AVFs (Figure 2B).

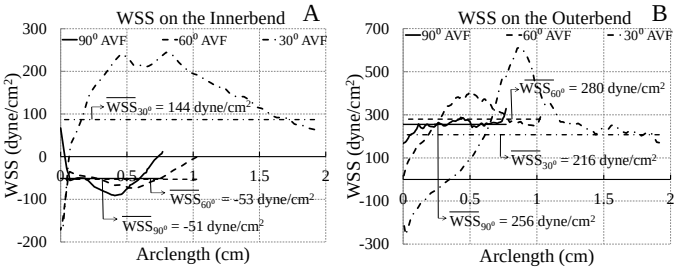

Figure 2. Axial WSS along A: the inner wall and B: the outer wall of the bend for the 90°, 60°, 30° AVFs. For all AVF, arclength was calculated on the centerline starting from the anastomotic junction.

In Figure 3, the range of WSS along the bend (ΔWSS: the maximum difference between the local WSS values which measures the axial WSS gradient) for each configuration was plotted versus Dean number ($De = \sqrt{(D_{ov}/2R_c)}Re_{ov}$; where D_{ov}, Re_{ov}, and R_c are the outflow vein diameter, Reynolds number, and radius of curvature, respectively). The *De* describes the strength of secondary motions due to the curvature of the bend segment and was 354, 683, and 966 for 30°, 60°, and 90° AVFs, respectively. ΔWSS was inversely correlated with *De* on the IW and OW. On the IW, ΔWSS was 414 dyne/cm^2, 170 dyne/cm^2, and 158 dyne/cm^2 for the 30°, 60°, and 90° AVFs, respectively. Similarly, ΔWSS was 870 dyne/cm^2, 405 dyne/cm^2, and 161 dyne/cm^2 on the OW of the 30°, 60°, and 90° AVFs.

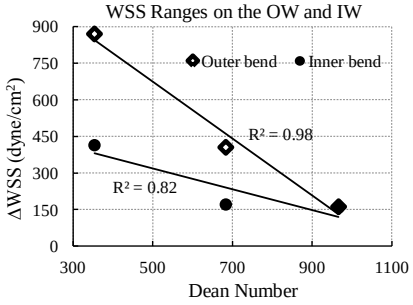

Figure 3. Maximum local variation in WSS for both the inner and outer walls of the bend for each of the three AVFs with their corresponding Dean number.

DISCUSSION AND CONCLUSIONS

The effects of the anastomotic angle on the WSS profile in AVFs were studied. We found that the AVFs with sharper angles (30° AVF) experienced relatively greater variations in WSS along the bend segment and had larger magnitude of WSS. As extremely high WSS and a high spatial gradient of WSS can be detrimental to endothelial cells, the tighter bends with larger radius of curvature and thus lower *De* may experience more adverse hemodynamics. Also, by categorizing AVFs with *De*, given the geometry of a fistula, we could predict the consequent WSS parameters. Particularly, of the models studied, the 90° AVF experienced the smallest potentially harmful variations in axial WSS along the fistula, and so it seemed to have the most advantageous WSS profile. On the other hand, the extreme WSS values were more localized and confined in the 60° and 30° AVFs, but NH is more likely to develop in the steep gradients. Thus, the maturation of an AVF, as hindered by both the severity and spread of NH, can significantly be affected by the configuration of the fistula.

ACKNOWLEDGEMENTS

This work was funded by NSF Grant No. 0756921.

REFERENCES

1. Rajabi-Jaghargh, E. et al., 2012. Seminars in Dialysis.
2. Krishnamoorthy, M. K. et al., 2008. Kidney International,74, pp. 1410-1419.
3. Ene-Iordache, B. et al., 2011. Nephrol Dial Transplant, 27, pp. 358-368.